J|A|C|S
ARTICLES
Published on Web 09/27/2006

Thermal Denaturing of Mutant Lysozyme with Both the OPLSAA and the CHARMM Force Fields

Maria Eleftheriou,[†] Robert S. Germain,[†] Ajay K. Royyuru,[†] and Ruhong Zhou*[,†,‡]

Contribution from the Computational Biology Center, Deep Computing Institute, IBM Watson Research Center, Yorktown Heights, New York 10598, and Department of Chemistry, Columbia University, New York, New York 10027

Received February 9, 2006; E-mail: ruhongz@us.ibm.com

Abstract: Biomolecular simulations enabled by massively parallel supercomputers such as BlueGene/L promise to bridge the gap between the currently accessible simulation time scale and the experimental time scale for many important protein folding processes. In this study, molecular dynamics simulations were carried out for both the wild-type and the mutant hen lysozyme (TRP62GLY) to study the single mutation effect on lysozyme stability and misfolding. Our thermal denaturing simulations at 400−500 K with both the OPLSAA and the CHARMM force fields show that the mutant structure is indeed much less stable than the wild-type, which is consistent with the recent urea denaturing experiment (Dobson et al. *Science* **2002**, *295*, 1719−1722; *Nature* **2003**, *424*, 783−788). Detailed results also reveal that the single mutation TRP62GLY first induces the loss of native contacts in the β-domain region of the lysozyme protein at high temperatures, and then the unfolding process spreads into the α-domain region through Helix C. Even though the OPLSAA force field in general shows a more stable protein structure than does the CHARMM force field at high temperatures, the two force fields examined here display qualitatively similar results for the misfolding process, indicating that the thermal denaturing of the single mutation is robust and reproducible with various modern force fields.

1. Introduction

Understanding the mechanism behind fatal diseases such as Alzheimer's disease related to protein misfolding and amyloid formation is one of the most challenging and urgent problems remaining in molecular biology, as the world population ages at an unprecedented pace.[1−4] Recent experiments pioneered by Dobson and co-workers have shown that amyloids and fibrils can be formed not only from the traditional β-amyloid peptides but also from almost any protein, such as lysozyme, given the appropriate conditions.[1−4] This opened a new and exciting window of research into the mechanism behind Alzheimer's disease and other amyloidosis[1] related to protein misfolding. There is strong evidence showing that the aggregation and amyloid formation is related to the instability of these proteins such as lysozyme when some key mutations occur.[1,2] One recent experiment[2] shows an interesting new finding about the protein lysozyme (hen lysozyme) in which a single mutation, TRP62GLY, causes the protein to misfold due to the loss of key "long-range hydrophobic interactions". More mysteriously, the single mutation site TRP62 is on the surface, not inside the hydrophobic core. The authors speculated that this TRP62 residue might be within the nucleation region during the folding process and then pushed to the surface for functional reasons. However, not many details were offered on how the key long-range hydrophobic interactions are lost and how the TRP62 residue is pushed from the nucleation region to the surface region.[2]

To understand the mechanism behind amyloid formation triggered by a single residue mutation, we performed molecular dynamics (MD) simulations for both the wild-type and the mutant lysozyme. Computer simulations performed at various levels of complexity, ranging from simple lattice models to all-atom models with explicit solvent, can be used to supplement experiment and fill in some of the gaps in our knowledge about protein folding pathways and intermediates, which are often inaccessible even from the current most sophisticated experimental approaches.[5−15] We believe that the combination of sophisticated experiments and the state-of-art molecular simulations may lead to a better understanding of the protein folding and misfolding mechanism.[5]

[†] IBM Watson Research Center.
[‡] Columbia University.

(1) Kagan, B. L.; Dobson, C. M. *Science* **2005**, *307*, 42−43.
(2) Klein-Seetharaman, J.; Oikawa, M.; Grimshaw, S. B.; Wirmer, J.; Duchardt, E.; Ueda, T.; Imoto, T.; Smith, L. J.; Dobson, C. M.; Schwalbe, H. *Science* **2002**, *295*, 1719−1722.
(3) Dumoulin, M.; Last, A.; Desmyter, A.; Decanniere, K.; Canet, D.; Spencer, A.; Archer, D.; Muyldermans, S.; Wyns, L.; Matagne, A.; Redfield, C.; Robinson, C.; Dobson, C. M. *Nature* **2003**, *424*, 783−788.
(4) Chiti, F.; Stefani, M.; Taddei, N.; Ramponi, G.; Dobson, C. M. *Nature* **2003**, *424*, 805−808.
(5) Fersht, A. R.; Daggett, V. *Cell* **2002**, *108*, 573−582.
(6) Fersht, A. R. *Structure and Mechanism in Protein Science*; W. H. Freeman and Co.: New York, 1999.
(7) Brooks, C. L.; Onuchic, J. N.; Wales, D. J. *Science* **2001**, *293*, 612−613.
(8) Dobson, C. M.; Sali, A.; Karplus, M. *Angew. Chem., Int. Ed.* **1998**, *37*, 868−893.
(9) Brooks, C. L.; Gruebele, M.; Onuchic, J. N.; Wolynes, P. G. *Proc. Natl. Acad. Sci. U.S.A.* **1998**, *95*, 11037.
(10) Duan, Y.; Kollman, P. A. *Science* **1998**, *282*, 740.
(11) Zhou, R.; Huang, X.; Margulius, C. J.; Berne, B. J. *Science* **2004**, *305*, 1605−1609.
(12) Liu, P.; Huang, X.; Zhou, R.; Berne, B. J. *Nature* **2005**, *437*, 159−162.
(13) Snow, C. D.; Nguyen, H.; Pande, V. S.; Gruebele, M. *Nature* **2002**, *420*, 102.
(14) Garcia, A. E.; Onuchic, J. N. *Proc. Natl. Acad. Sci. U.S.A.* **2003**, *100*, 13898−13903.
(15) Kokubo, H.; Okamoto, Y. *Chem. Phys. Lett.* **2004**, *392*, 168−175.

10.1021/ja060972s CCC: $33.50

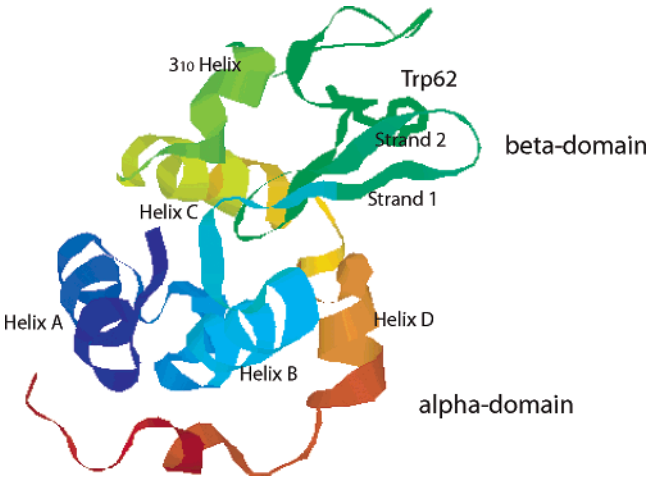

Figure 1. A ribbon view of the native lysozyme protein, with residue Trp62 represented in sticks and both α- and *β*-domains marked in the figure.

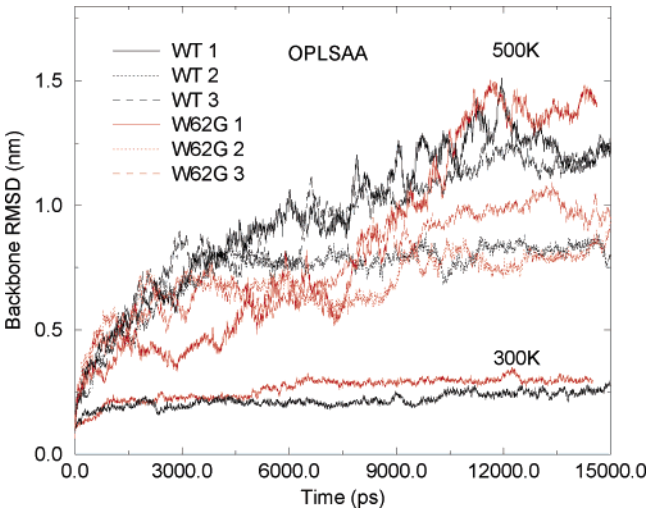

Figure 2. Comparison of all backbone RMSDs from the starting crystal structures for both the wild-type and the mutant trajectories, with three trajectories each for the wild-type and mutant lysozyme. The results are obtained from the 500 K NVT simulations with the OPLSAA force field. Overall, these trajectories show RMSDs comparable to those of the initial structures.

The experimental time scale of protein folding even for modest sized proteins is often on the order of microseconds to milliseconds, which implies that brute force molecular dynamics simulations of protein folding, although starting to become accessible, will still take many months or even years on modern supercomputers. The current simulations were done on a prototype BlueGene/L machine with 512 nodes. Thus, we utilized the thermal denaturation method[16−18] at very high temperatures, such as 400−500 K, to promote unfolding in molecular dynamics. It should be noted that this technique might introduce a distorted (un)folding free energy landscape due to the larger entropic contributions at higher temperatures. Nevertheless, the thermal denaturation simulations do offer a quick and straightforward way to address the mechanism behind the protein stability and misfolding, as we are going to see in the following sections. Now that more hardware resources have become available, we are currently running simulations of lysozyme in 8 M urea solutions to mimic the chemical denaturation experiments.[2] The results from the urea solution simulations will be presented elsewhere.

This paper is organized as follows. The lysozyme wild-type and mutant systems and computational methods are described in section 2. Section 3 gives detailed simulation results from both the OPLSAA and the CHARMM force fields. The last section provides the conclusion and remarks for future directions. The current work demonstrates that much can be learned from these high temperature thermal denaturation simulations.

2. Systems and Methods

The starting structure of the wild-type protein, the hen lysozyme, in our simulations is taken from the crystal structure deposited in the PDB (193L), as shown in Figure 1. The wild-type lysozyme protein contains two structural domains, the α-domain, involving residues 1−35 and 85−129, and the *β*-domain, which comprises residues 36−84. It has four α-helices (Helix A (5−14), Helix B (25−36), Helix C (90−100), and Helix D (110−115)), two *β*-strands (Strand 1 (43−46), Strand 2 (51−54)), and a loop (60−78) region, as well as a 3_{10}-helix (81−85). The mutation site TRP62 is in the loop region, and the starting structure for the mutant was generated by a single residue replacement, TRP62GLY, from the wild-type structure. The resulting protein configurations are then solvated in a water box of size 60 × 60 × 60 Å^3. Eight Cl^- counterions are added to neutralize both solvated systems. The solvated protein systems have about 21 000 atoms. Both the OPLSAA force field[19] together with a SPC water model,[20] and the CHARMM (charmm22) force field[21] with a modified TIP3P water model,[22,23] are used for the simulation. For the long-range electrostatic interactions, we make use of the Particle-Particle Particle-Mesh Ewald (P3ME) method,[24] while for the van der Waals interactions, a typical 10 Å cutoff is used.

A standard equilibration procedure is adopted for both the wild-type and the mutant protein systems. It starts with a conjugate gradient minimization for each solvated system. Next, a two-stage equilibration, each consisting of 100 ps MD, is followed: in the first stage, the protein is frozen in space and only the solvent molecules are equilibrated; in the second stage, all atoms are equilibrated. The configurations from the above two-stage equilibration are then used as the starting points for another 1000 ps NPT simulation at 300 K and 1 atm. Three configurations are picked from the last 300 ps trajectory, each 100 ps apart, as the final starting configurations. Thus, for both the wild-type and the mutant lysozyme, three trajectories starting from different initial configurations are performed.

For each configuration (total six, three for the wild-type and three for the mutant), five different temperatures, 300, 350, 400, 450, and 500 K, are used for simulation with up to 15 ns MD each. For most of the results reported in the following, the higher temperature thermal denaturing simulations are used due to the fact that the lower temperature simulations, such as those at 300 and 350 K, had little structural change during the simulation. These simulations are done with the NVT ensemble with the temperature controlled by the Anderson thermostat.[25] A time step of 1.0 fs is used with bond lengths constrained for all simulations.

We used the BlueMatter application framework[26] for the simulation of these systems. BlueMatter is a molecular dynamics application framework developed in conjunction with the BlueGene/L hardware.[27] The major goal of this application is to achieve strong scalability on massively parallel machines such as the BlueGene/L supercomputer to support research on protein folding and related areas, which require long biomolecular simulations on a modest size range of systems (10 000−100 000 particles). All of the simulations presented in this paper were carried out with the IBM BlueGene/L prototype machine with 512 nodes running in parallel.

3. Results and Discussion

We first simulated both the wild-type and the TRP62GLY mutant lysozyme at 300 K to see if the protein structure stays folded during our simulation length. Indeed, at 300 K, we

(16) Daggett, V.; M., L. *Mol. Biol.* **1994**, *232*, 600.
(17) Daggett, V. *Curr. Opin. Struct. Biol.* **2000**, *10*, 160.
(18) Brooks, C. L. *Curr. Opin. Struct. Biol.* **1998**, *8*, 222.

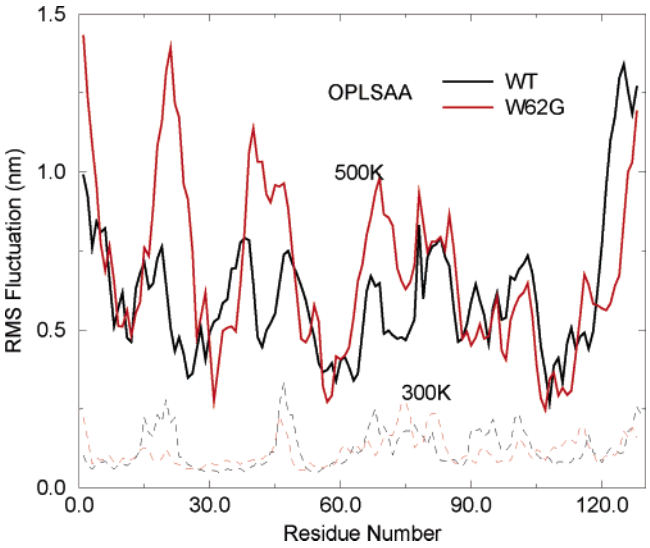

Figure 3. Comparison of the RMS fluctuation for the wild-type and mutant lysozyme. The results are obtained from the 500 K NVT simulations with the OPLSAA force field. Even though the two RMSDs do not show much difference, the RMS fluctuations show that the mutant lysozyme has much larger fluctuations near residues in the β-domain.

observe that the RMSD based on the backbone atoms plateaus around 2−3 Å from the crystal structure during the 15 ns simulation (see Figure 2), indicating the force field is reasonable in terms of the protein stability (CHARMM force field shows similar results, see below). This stability also agrees with the previous simulations on lysozyme at 300 K by Goodfellow et al.[28] For the OPLSAA force field, the lysozyme protein, both the wild-type and the mutant, stays fairly stable up to 400 K with an RMSD less than 4−5 Å during the entire 15 ns MD simulation. Only when the temperature increases to 450−500 K does the protein start to unfold (see Supporting Information). On the other hand, with the CHARMM force field, the protein starts to unfold around 400 K within the 15 ns MD simulation (see Supporting Information). Thus, the OPLSAA force field seems to show more stable structures at high temperatures than does the CHARMM force field. This is probably due to larger energy barriers, such as from backbone torsions, in the OPLSAA force field than in the CHARMM (charmm22) force field. This relatively higher stability of the OPLSAA force field than the CHARMM (charmm22) force field has been found previously as well in dipeptide conformational distributions[29] and at β-hairpin folding melting temperatures.[30,31] Thus, in the following, we present thermal denaturing results from 500 K for the OPLSAA force field and 400 K for the CHARMM force field, each with three 15 ns trajectories starting from different initial configurations described in the above methods section.

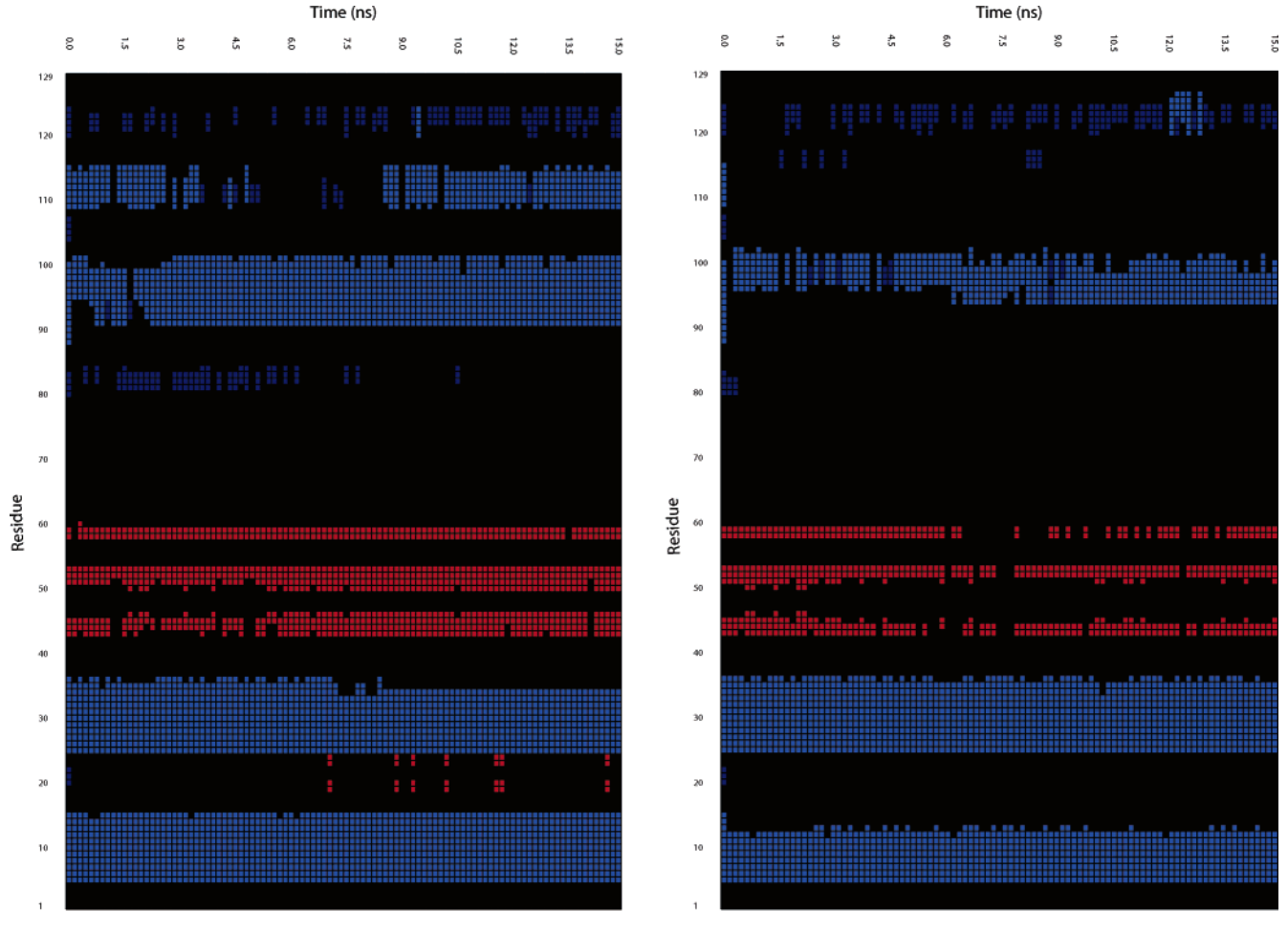

(a) wild-type (b) mutant

Figure 4. Time-evolution of the secondary structure at 300 K (with OPLSAA force field). (a) Wild-type and (b) Trp62Gly mutant. The secondary structure is assigned by the program STRIDE,[34] with α-helix colored blue, 3_{10} colored light blue, β-strand colored red, and coils colored black. The secondary structure of the starting crystal structure is displayed at $t = 0$ ns (Helix A (5−14), Helix B (25−36), Helix C (90−100), Helix D (110−115), Strand 1 (43−46), Strand 2 (51−54), and a 3_{10}-helix (81−85)).

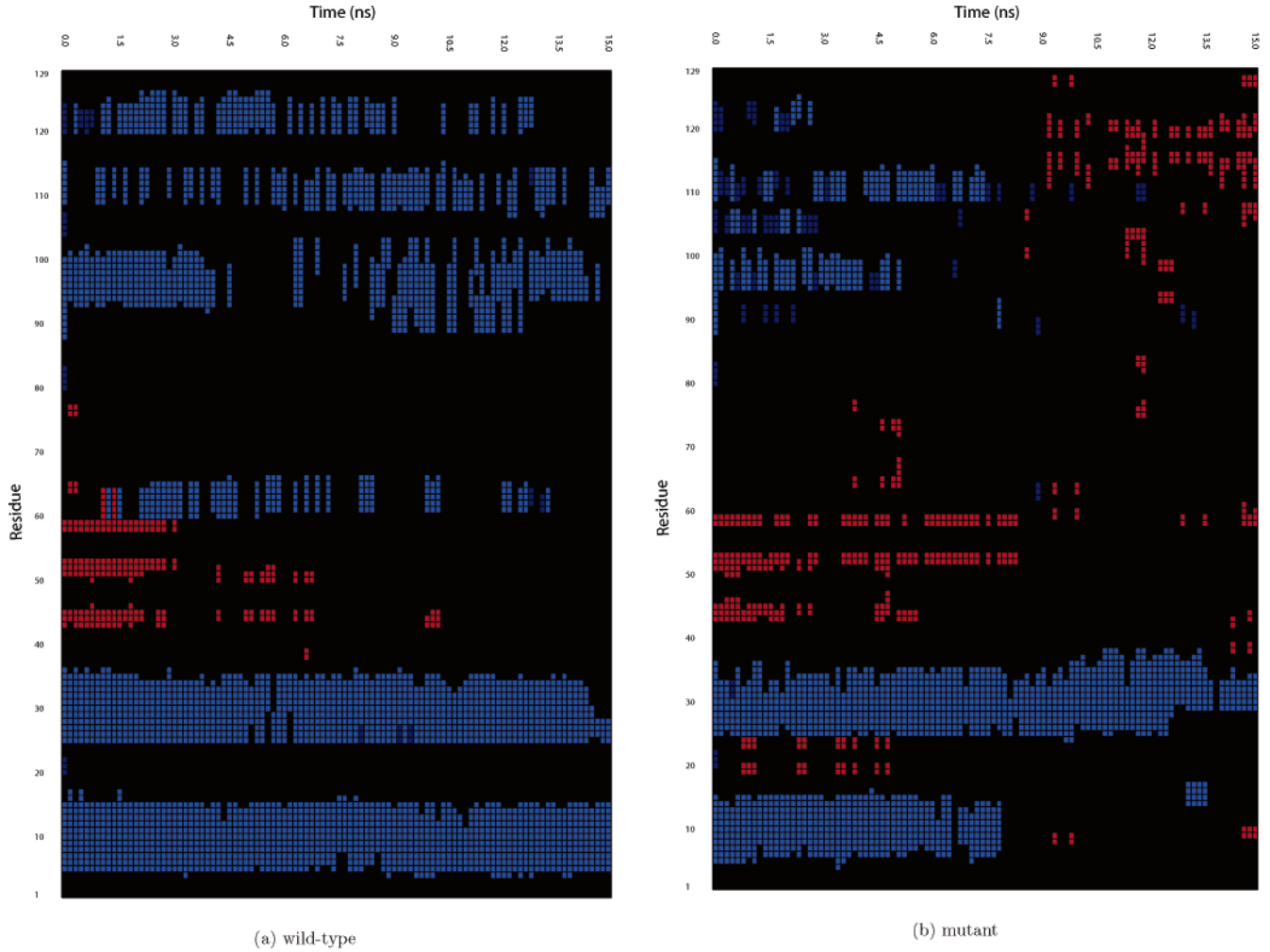

Figure 5. Time-evolution of the secondary structure at 500 K (with OPLSAA force field). (a) Wild-type and (b) Trp62Gly mutant. See the legend to Figure 4 for further details.

3.1. Thermal Denaturation with the OPLSAA Force Field. Global Behavior. Figure 2 shows the comparison of backbone RMSDs from the crystal structures for both the wild-type and the mutant lysozyme. These trajectories (total six, three from the wild-type and three from the mutant) are from simulations with the OPLSAA field at 500 K (the RMSDs from the control runs at 300 K are also shown in Figure 2; these control runs show that both the wild-type and the mutant are very stable at room temperature). Overall, these trajectories show a steady increase in RMSD during the 15 ns simulation. The results also show a comparable RMSD for both the wild-type and the mutant, with the mutant having slightly higher RMSDs (see more below for the CHARMM force field). As was pointed out before,[32] overall RMSD might not be a good measure of the local structures when the RMSD values go beyond a certain value, for example, 8 Å. Comparable RMSD values might show very different local or nonlocal contacts. Nevertheless, the large RMSD values (≥10 Å) do indicate that the protein structures are largely denatured after 15 ns at these high temperatures. It is interesting to note that our results are consistent with those of Goodfellow and co-workers.[28] These authors also found comparable RMSDs in their 5 ns thermal denaturing simulations at 500 K for the wild-type and mutant of human lysozyme.[28]

The root-mean-square fluctuations (RMSF) of the atoms across all of the simulations of the wild-type and mutant lysozyme are thus further calculated for the C_α atoms to characterize the local fluctuations. Figure 3 shows the comparison of the RMSF for the wild-type and mutant lysozyme using the same trajectory data from the OPLSAA force field at 500 K (again the 300 K control data are also shown). Even though the RMSDs do not show much difference, the RMS

(19) Jorgensen, W. L.; Maxwell, D.; Tirado-Rives, J. *J. Am. Chem. Soc.* **1996**, *118*, 11225−11236.
(20) Berendsen, H. J. C.; Postma, J. P. M.; van Gunsteren, W. F.; Hermans, J. In *Intermolecular Forces*; Pullman, B., Ed.; Reidel: Dordrecht, 1981; pp 331−342.
(21) Brooks, B. R.; Bruccoeri, R. E.; Olafson, B. D.; States, D. J.; Swaminathan, S.; Karplus, M. *J. Comput. Chem.* **1983**, *4*, 187.
(22) Neria, E.; Fischer, S.; Karplus, M. *J. Chem. Phys.* **1996**, *105*, 1902−1921.
(23) Jorgensen, W. L.; Chandrasekhar, J.; Madura, J.; Impey, R. W.; Klein, M. L. *J. Chem. Phys.* **1983**, *79*, 926−935.
(24) Essman, U.; Perera, L.; Berkowitz, M. L.; Darden, T.; Lee, H.; Pedersen, L. G. *J. Chem. Phys.* **1995**, *103*, 8577.
(25) Swope, W. C.; Anderson, H. C.; Berens, P. H.; Wilson, K. R. *J. Chem. Phys.* **1982**, *76*, 637.
(26) Fitch, B. G.; Germain, R. S.; Mendell, M.; Pitera, J.; Pitman, M.; Rayshubskiy, A.; Sham, Y.; Suits, F.; Swope, W.; Ward, T. J.; Zhestkov, Y.; Zhou, R. *J. Parallel Distri. Comput.* **2003**, *63*, 759−773.
(27) Allen, F.; et al. *IBM Syst. J.* **2001**, *40*, 310−327.
(28) Moraitakis, G.; Goodfellow, J. *Biophys. J.* **2003**, *84*, 2149−2158.
(29) Hu, H.; Elstner, M.; Hermans, J. *Proteins* **2003**, *50*, 451−463.
(30) Dinner, A. R.; Lazaridis, T.; Karplus, M. *Proc. Natl. Acad. Sci. U.S.A.* **1999**, *96*, 9068−9073.
(31) Zhou, R.; Berne, B. J.; Germain, R. *Proc. Natl. Acad. Sci. U.S.A.* **2001**, *98*, 14931−14936.
(32) Venclovas, C.; Zenla, A.; Fidelis, K.; Moult, J. *Proteins* **1999**, *S3*, 231−237.

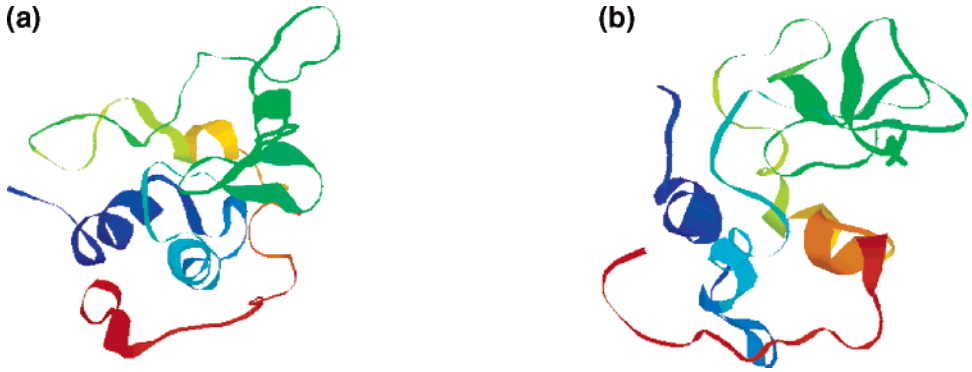

Figure 6. Representative structures from the clustering analysis for both the wild-type (a) and the mutant (b) lysozyme (residue 62 represented by sticks). The results are again obtained from the 500 K NVT simulations with the OPLSAA force field. The mutant lysozyme shows a more disrupted β-domain region, indicating more loss of the native contacts in the mutant than in the wild-type. This is particularly true in the β-domain region.

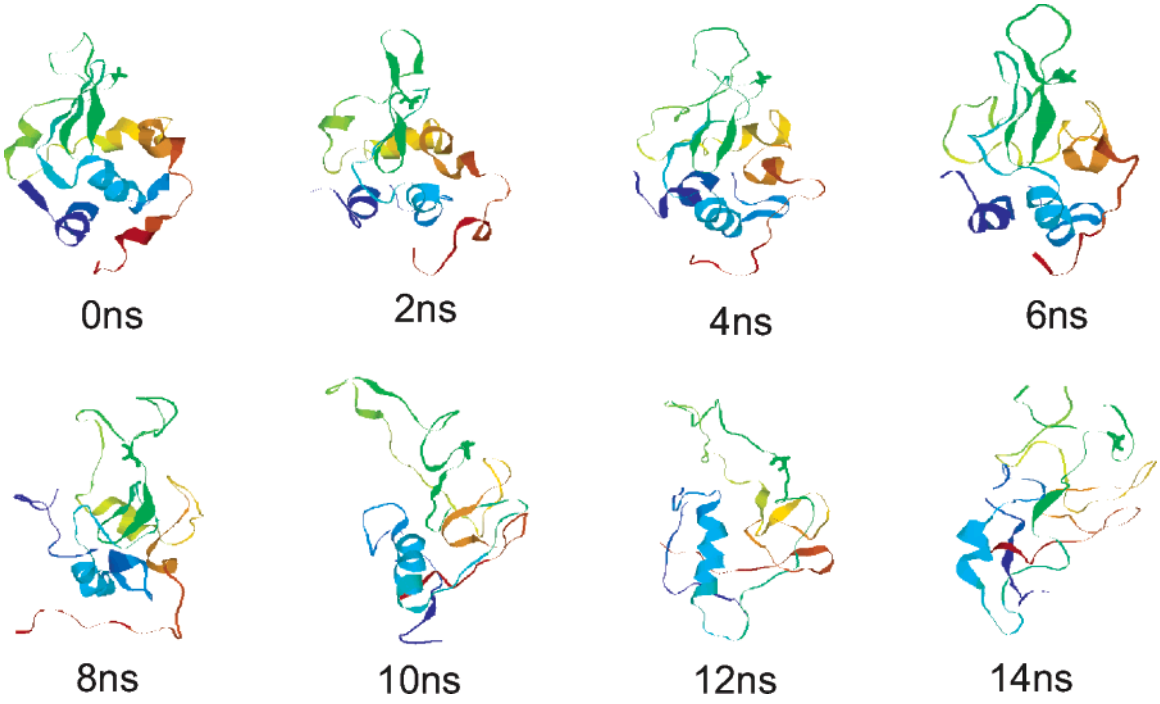

Figure 7. Snapshots of the mutant lysozyme at 0, 2, 4, 6, 8, 10, 12, and 14 ns during one of the 500 K trajectories with the OPLSAA force field. These snapshots clearly indicate the gradual loss of the native contacts, with most of the loss in the β-domain first.

fluctuations, on the other hand, do show much of the difference; the mutant lysozyme has much larger fluctuations than does the wild-type. We observe that during unfolding the mutant tends to have higher fluctuations in some of the regions. This difference is most notable in the β-domain and, in particular, in the loop region where the mutation site TRP62 resides. This loop region also displays a larger fluctuation even at lower temperatures such as 350−400 K for the mutant. Such behavior might not be too surprising as the hydrogen-bonding network connecting this loop region with the two β-strands, Strand 1 (residues 43−46) and Strand 2 (residues 51−54), in the wild-type is disrupted due to the mutation, thus leading to a more unrestrained motion of the loop. Figures 4 and 5 show the time-evolution of the secondary structure[33] for both the wild-type and the mutant lysozyme at 300 K (control run) and 500 K, respectively. The secondary structures are obtained from the program STRIDE.[34] Overall, the 300 K simulations show a fairly stable trajectory of all secondary structure components, with the mutant showing slight disruptions in the β-strands. Another interesting point to notice is that Helix D in the wild-type transiently unfolds around 5−8 ns, and then refolds back to α-helix, indicating that Helix D might be flexible. It is also possible that this is an artifact of the force field. The 500 K simulations, particularly the mutant, show a large disruption in the secondary structures. Overall, the disruptions in the mutant are largely from the β-domain region as well as Helix C (residue 90−100) in the α-domain region. Some non-native short β-strands also appear in the original Helix C and Helix D region once unfolded (more secondary structure trajectories are shown in the Supporting Information; even though each individual trajectory does show slightly different behavior, overall they still show a reasonably good consensus in terms of secondary structure deformation and reformation). These disruptions of secondary structures, as well as the higher fluctuations and thus lower stability in the mutant, seem to agree well with the experiment in general, where the authors[2] found that the single mutation TRP62GLY caused the

(33) de Bakker, P. I.; Hunenberger, P. H.; McCammon, J. A. *J. Mol. Biol.* **1999**, *285*, 1811−1830.
(34) Frishman, D.; Argos, P. *Proteins* **1995**, *23*, 566−579.

nativelike contacts, some long-range, in the wild-type to disappear in highly denaturing 8 M urea solution. However, the authors did not identify the origin and/or the order of the disruptions in this case, probably due to the experimental resolution limit. More experiments on this misfolding process might prove to be extremely useful here.

Representative Structures. It is of great interest to take a closer look at the representative structures during the wild-type and mutant lysozyme unfolding, because they might reveal important information about the cause of the different behavior. The representative structures for both the wild-type and the mutant are obtained by the clustering analysis with the 5−15 ns trajectory data (the first 5 ns was omitted in clustering analysis due to the fact that they resemble the nativelike starting structures).[31,35] In the current clustering method, a distance matrix based on the backbone RMSD was first calculated. Next, by counting the number of neighbors within a cutoff of 2.0 Å, we eliminated the structure with the largest number of neighbors (representative structure) and all its neighbors as a cluster from the pool. We repeated this for the remaining structures in the pool until no structures were left.[31,35] Figure 6 shows the representative structures for both the wild-type and the mutant. As expected, the mutant shows more disrupted β-strands in the representative structure than does the wild-type, indicating a much more significant loss of the native contacts in the mutant than in the wild-type. This is particularly true in the β-domain region and Helix C of the α-domain.

Unfolding Trajectory. To see how the mutant loses its nativelike contacts during the thermal denaturing process, it is useful to look at some detailed snapshots in the unfolding trajectory. Figure 7 shows snapshots of the mutant at 0, 2, 4, 6, 8, 10, 12, and 14 ns from one of the three 500 K trajectories with the OPLSAA force field. The first major unfolding event happens around 4 ns, when Strand 1 (residues 43−46) starts to disappear in the mutant (it should be noted that this is MD simulation time at high temperature, not the real unfolding time at biological temperature). Interestingly, Helix C (residues 90−100) is also partially destroyed during this time period. When time moves on, Strand 2 (residues 51−54) begins to show large fluctuations and then disappears around 9−10 ns. At this point, basically the nativelike local contacts (secondary structures) in the β-domain are largely destroyed. Meanwhile, Helix B (residues 25−36) in the α-domain is intact, while Helix C (residues 90−100) and Helix D (residues 110−115), on the other hand, are turned into some kind of non-native short β-strands, indicating a large disruption in its local contacts. At the end of the 15 ns simulation, the α-domain structures start to be largely destroyed as well. The protein is essentially in a molten-globule structure with a significantly larger radius of gyration; the radius of gyration increased from 14.3 Å at 0 ns to ∼17.0 Å at 15 ns. These results indicate that the unfolding process starts at the β-domain region, with the two β-strands being destroyed first, then adjacent Helix C and Helix D, and then the α-domain. Other trajectories show similar results even though the exact time for each unfolding event is slightly different (see Supporting Information on various time-evolutions of secondary structures).

3.2. Thermal Denaturation with the CHARMM Force Field. As mentioned earlier, the CHARMM force field results, in general, show less stable protein structures at higher temperatures than do the results of the OPLSAA force field. Thus, in the following, we use data from 400 K for illustration, which show roughly the same RMSD ranges as the 500 K in the OPLSAA force field. Figure 8a shows the comparison of the backbone RMSDs for the wild-type and mutant lysozyme from the CHARMM simulations at 400 K (with RMSDs at 300 K control runs also shown), and Figure 8b shows the comparison of the RMS fluctuations for the wild-type and mutant lysozyme (again with control run data at 300 K also shown). Figure 9shows the time-evolution of the secondary structure for both the wild-type and the mutant lysozyme at 400 K. Similarly, the mutant displays a larger fluctuation and a more disrupted secondary structure than does the wild-type. In this case, the mutant also displays a faster increase in RMSD than does the native structure, as shown in Figure 8a. These results show that indeed the mutant lysozyme is much less stable than the wild-type (more results on the time-evolution of secondary structures are shown in the Supporting Information). Figure 10 shows the representative structures from the same clustering analysis for both the wild-type and the mutant lysozyme. The results again

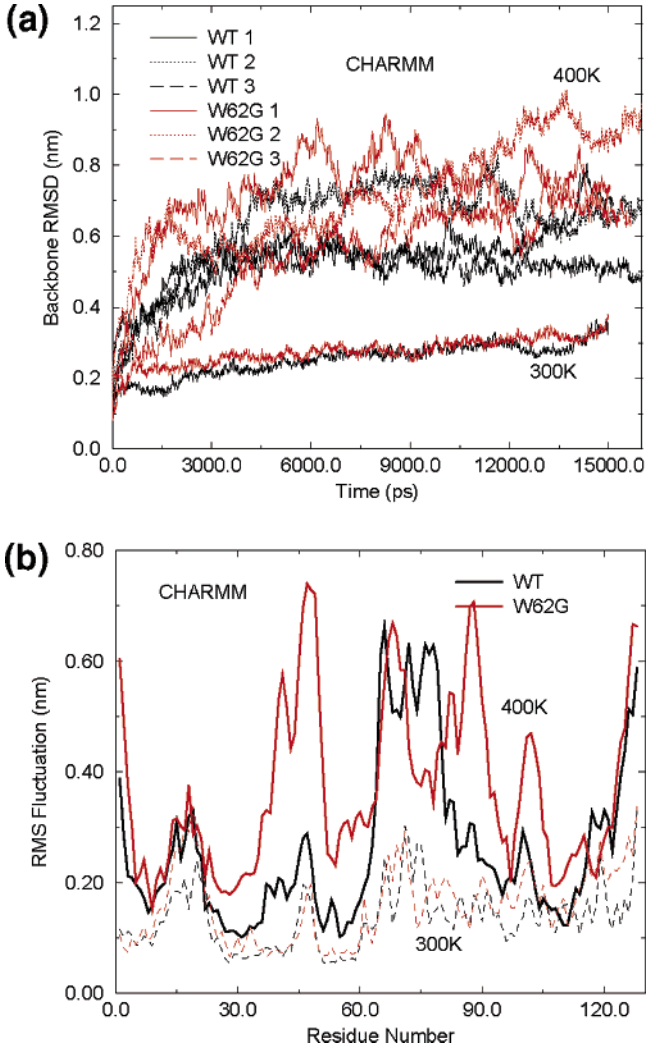

Figure 8. (a) Comparison of the backbone RMSD for the wild-type and mutant lysozyme from one representative trajectory. (b) Comparison of the RMS fluctuation for the wild-type and mutant lysozyme. The results are obtained from the 400 K NVT simulations with the CHARMM force field. In this case, both the backbone RMSD and the RMS fluctuations show that the mutant lysozyme has much larger deviations from the initial crystal structure.

(35) Zhou, R. *Proc. Natl. Acad. Sci. U.S.A.* **2003**, *100*, 13280−13285.

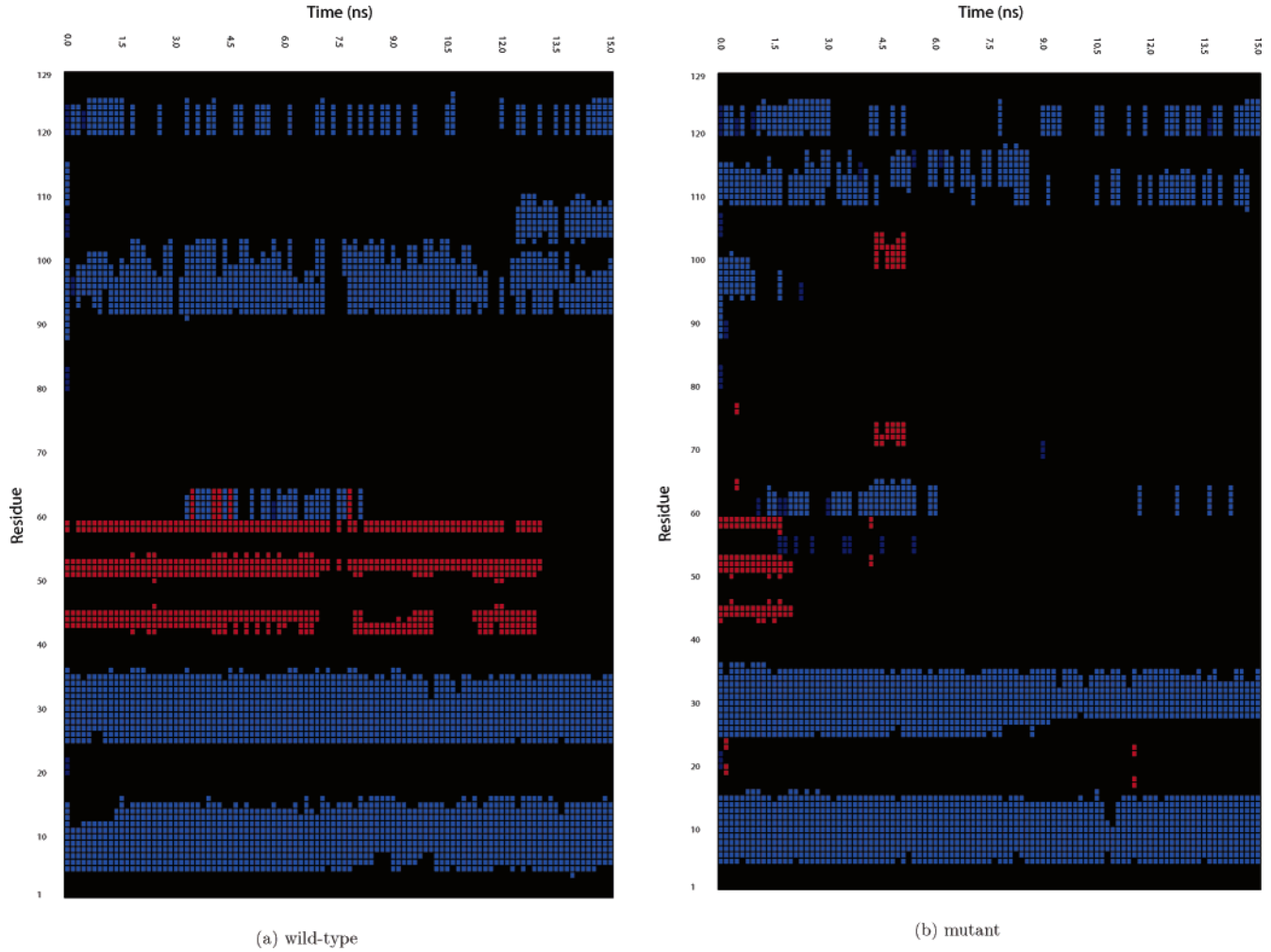

Figure 9. Time-evolution of the secondary structure at 400 K with the CHARMM force field. (a) Wild-type and (b) Trp62Gly mutant. See the legend to Figure 4 for further details.

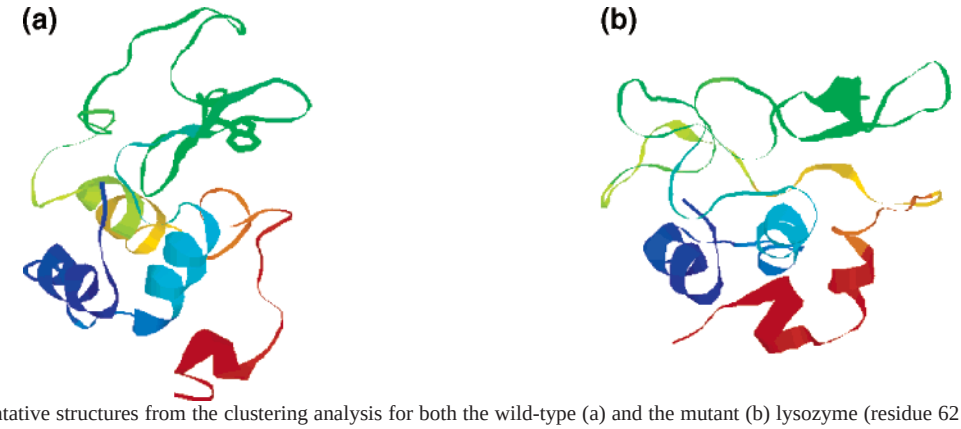

Figure 10. Representative structures from the clustering analysis for both the wild-type (a) and the mutant (b) lysozyme (residue 62 represented by sticks). The results are again obtained from the 400 K NVT simulations with the CHARMM force field. The mutant lysozyme shows a more disrupted β-domain region, indicating more loss of the native contacts in the mutant than in the wild-type. This is particularly true in the β-domain region.

reveal a more disrupted β-domain region as well as a destroyed Helix C of the α-domain in the mutant, indicating a much more significant loss of the native contacts in the β-domain region in the mutant than in the wild-type. The native-contact loss spreads from the β-domain region into Helix C of the α-domain region and then to other helices, as the unfolding proceeds. It is also interesting to note the slight differences in the results from the OPLSAA and CHARMM force fields. Basically, the OPLSAA force field prefers some non-native short β-strands in both the original β-domain and the α-domain's Helix C region after being unfolded, while the CHARMM force field prefers more of a random coil in the original β-domain after being unfolded. However, both force fields show that the misfolding/unfolding starts at the β-domain, and then spreads into Helix C of the α-domain region.

4. Conclusion

In this paper, we have studied the single mutation effect on the stability and misfolding of the protein lysozyme using

molecular dynamics simulations. Both the wild-type and the mutant lysozyme (TRP62GLY) were simulated on a 512-processor BlueGene/L prototype machine with two different force fields, OPLSAA and CHARMM. Our results from the thermal denaturing simulations at 400−500 K show that the mutant structure is indeed much less stable than the wild-type structure, which is consistent with the recent urea denaturing experiment.[2] Detailed results also reveal that the single mutation TRP62GLY first induces the loss of native contacts in the β-domain region of the lysozyme protein at high temperatures, and then the unfolding spreads into Helix C of the α-domain region. The two force fields examined here show comparable results in terms of denaturing procedure for the mutant, even though overall the OPLSAA force field shows more stable structures than does the CHARMM force field at high temperatures. The thermal denaturing results at various temperatures examined, 300, 350, 400, 450, and 500 K, reveal that the OPLSAA force field at 450−500 K and the CHARMM force field at 400 K have roughly the same RMSDs and RMS fluctuations from the initial crystal structures. Nevertheless, the results from both force fields indicate that the thermal denaturing of the single mutation is robust and reproducible with various modern force fields, although the absolute energy scales, such as energy barriers, may differ. These results might offer some indication in understanding the mechanism behind the protein misfolding and amyloid formation.

Acknowledgment. We would like to acknowledge the contributions of the people who have participated in the development of the BlueMatter code, including Blake G. Fitch, Aleksandr Rayshubskiy, Frank Suits, Yuri Zhestkov, T. J. Chris Ward, Mike Pitman, Jed Pitera, and Bill Swope. We would like to thank Bruce Berne and Chris Dobson for many helpful discussions. We would also like to acknowledge the contributions of the BlueGene/L hardware and system software teams, whose efforts and assistance made it possible for us to use the BlueGene/L prototype hardware.

Supporting Information Available: Additional figures showing backbone RMSD trajectories and secondary structure trajectories. This material is available free of charge via the Internet at http://pubs.acs.org.

JA060972S